Supplement of Weather Clim. Dynam., 7, 1009–1032, 2026
https://doi.org/10.5194/wcd-7-1009-2026-supplement


*Supplement of*

# Physical processes leading to extreme day-to-day temperature change – Part 2: Future climate change

**Kalpana Hamal and Stephan Pfahl**

*Correspondence to:* Kalpana Hamal (k.hamal@fu-berlin.de)

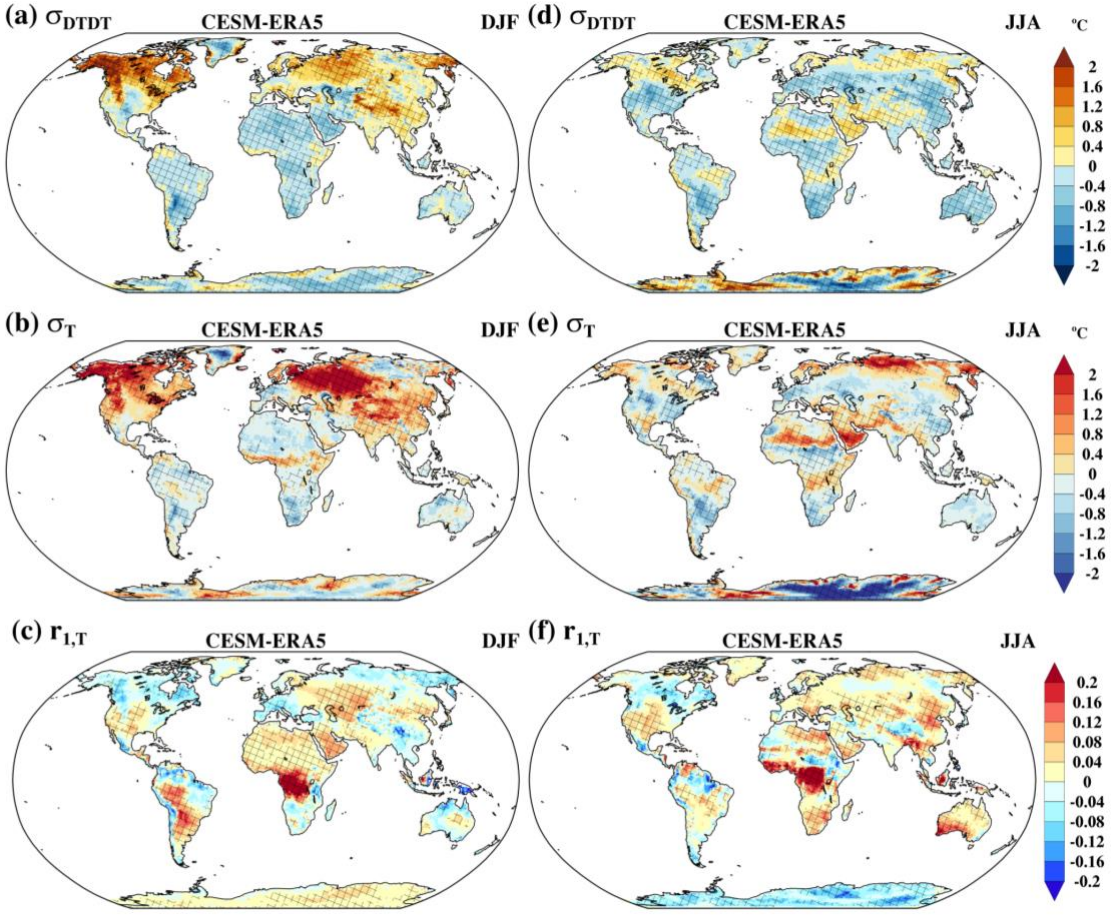


**Figure S1.** The differences between the CESM–LE and ERA5 of (**a, d**) standard deviation of DTDT variations ($\sigma_{DTDT}$, °C), (**b, e**) standard deviation of daily mean temperature ($\sigma_T$, °C), and (**c, f**) lag–1 autocorrelation of daily mean temperature ($r_{1,T}$) in December–February (DJF, **a–c**) and June–August (JJA, **d–f**). In panels (**a–f**), cross–hatching marks grid points where the CESM–LE ensemble mean differs significantly from the ERA5–derived metric, with statistical significance determined through bootstrap resampling.

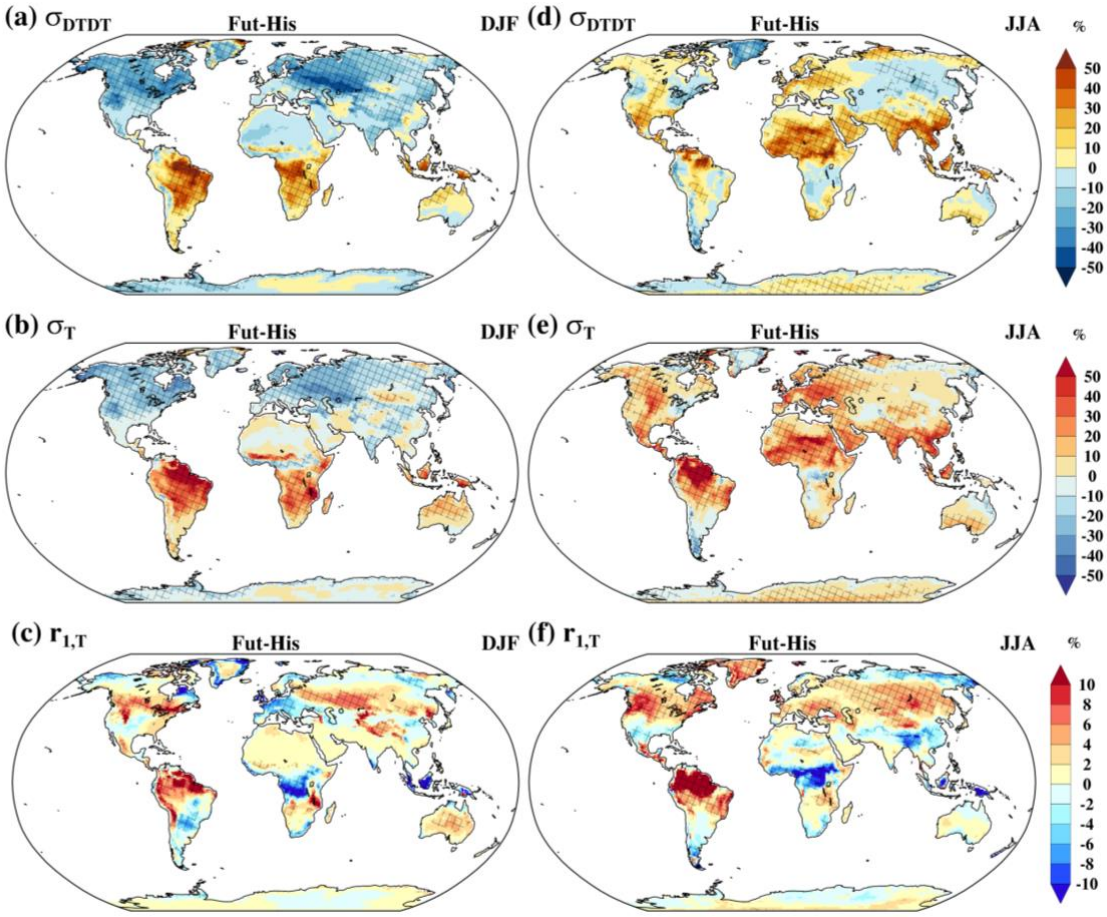


**Figure S2.** The projected percentage changes of (**a, d**) standard deviation of DTDT variations ($\sigma_{DTDT}$, %), (**b, e**) standard deviation of daily mean temperature ($\sigma_T$, %), and (**c, f**) lag–1 autocorrelation of daily mean temperature ($r_{1,T}$, %) in December–February (DJF, **a–c**) and June–August (JJA, **d–f**). In panels (**a–f**), cross–hatching denotes grid points where the future minus historical difference is significantly different from zero, assessed through bootstrapping.

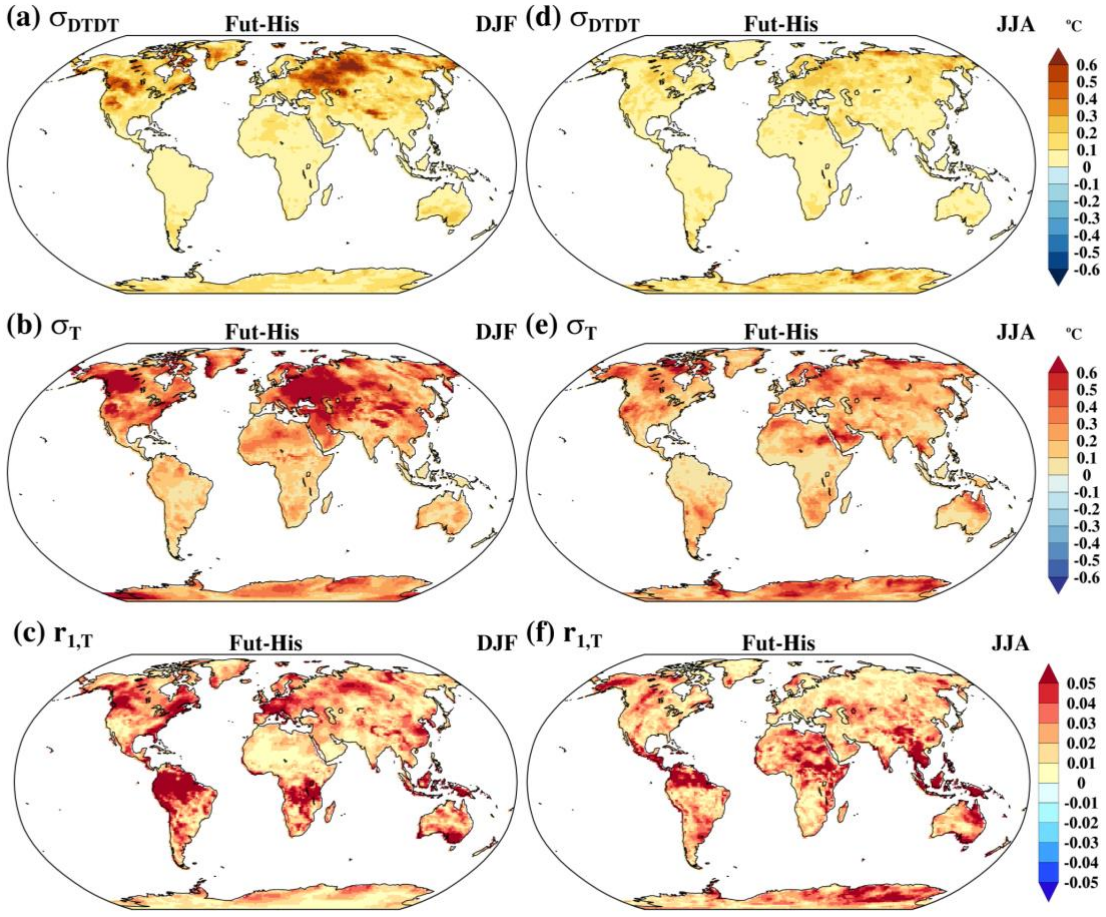


**Figure S3.** Intermodel variance (ensemble standard deviation) in the projected change of (**a, d**) standard deviation of DTDT variations ($\sigma_{DTDT}$, °C), (**b, e**) standard deviation of daily mean temperature ($\sigma_T$, °C), and (**c, f**) lag–1 autocorrelation of daily mean temperature ($r_{1,T}$) in December–February (DJF, **a–c**) and June–August (JJA, **d–f**).

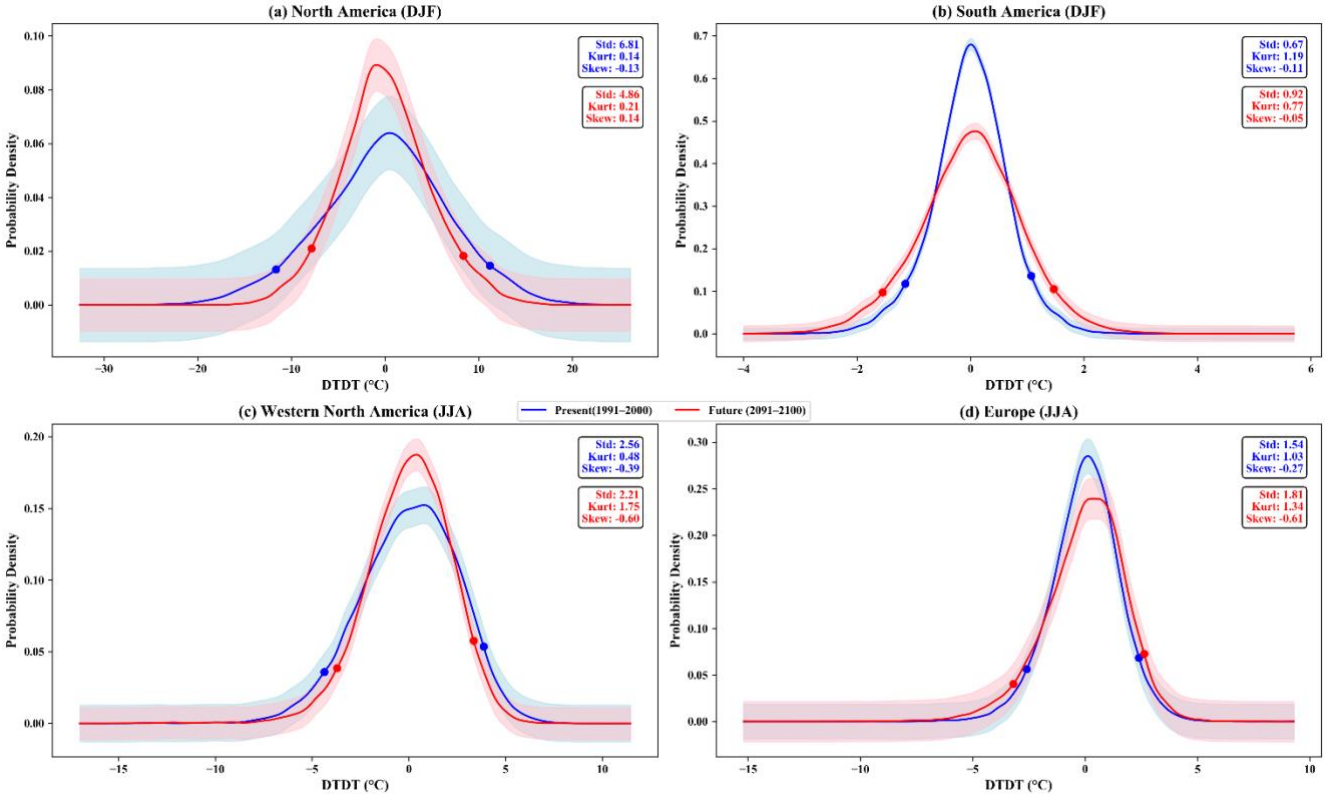


**Figure S4.** The DTDT change distribution curves over the selected locations: (**a**) North America, (**b**) tropical South America, (**c**) western North America, and (**d**) central Europe for December–February (DJF, **a–b**) and June–August (JJA, **c–d**). The blue and red curves represent the historical (1991–2000) and future (2091–2100) climates, respectively. The shading shows the 5–95% confidence interval. The small dots on the left and right represent the 5th and 95th percentiles, respectively.

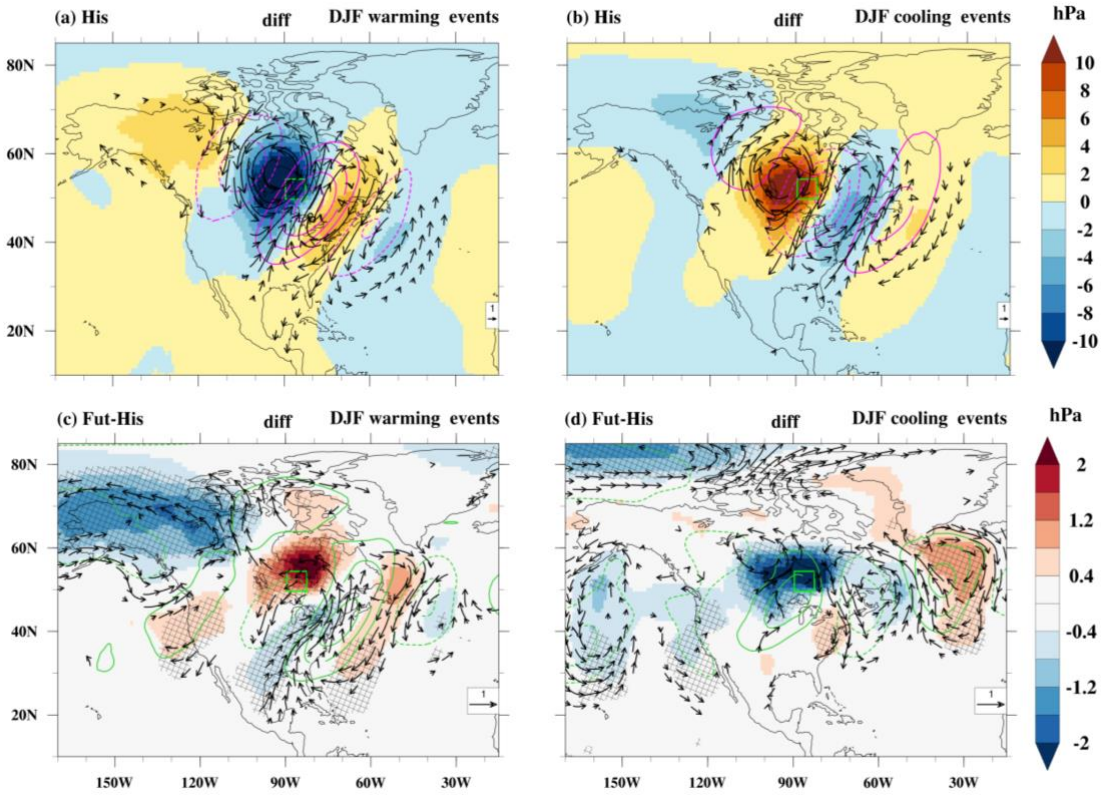


**Figure S5.** Composite difference of absolute sea level pressure (hPa, color shading), wind at 850 hPa (m $s^{-1}$ , vectors), and geopotential height 500 hPa (gpm, magenta and darkgreen contours) between the previous day (*t*–1) and event day (*t*) of the warming (**a, c**) and cooling (**b, d**) events during December–February (DJF) in historical climate (His, **a–b**) and projected changes (Fut–His, **c–d**) at a selected grid box in North America (green box). Note that (in **a–b**) wind vector anomalies ≥1.5 m $s^{-1}$ and (in **c–d**) wind vector anomalies ≥0.5 m $s^{-1}$ are plotted. The bold and dotted contours show increases and decreases of geopotential height, respectively. The cross–hatching area indicates where the ensemble mean of sea level pressure differences (Fut–His) exceeds the 95% confidence threshold based on a t–test.

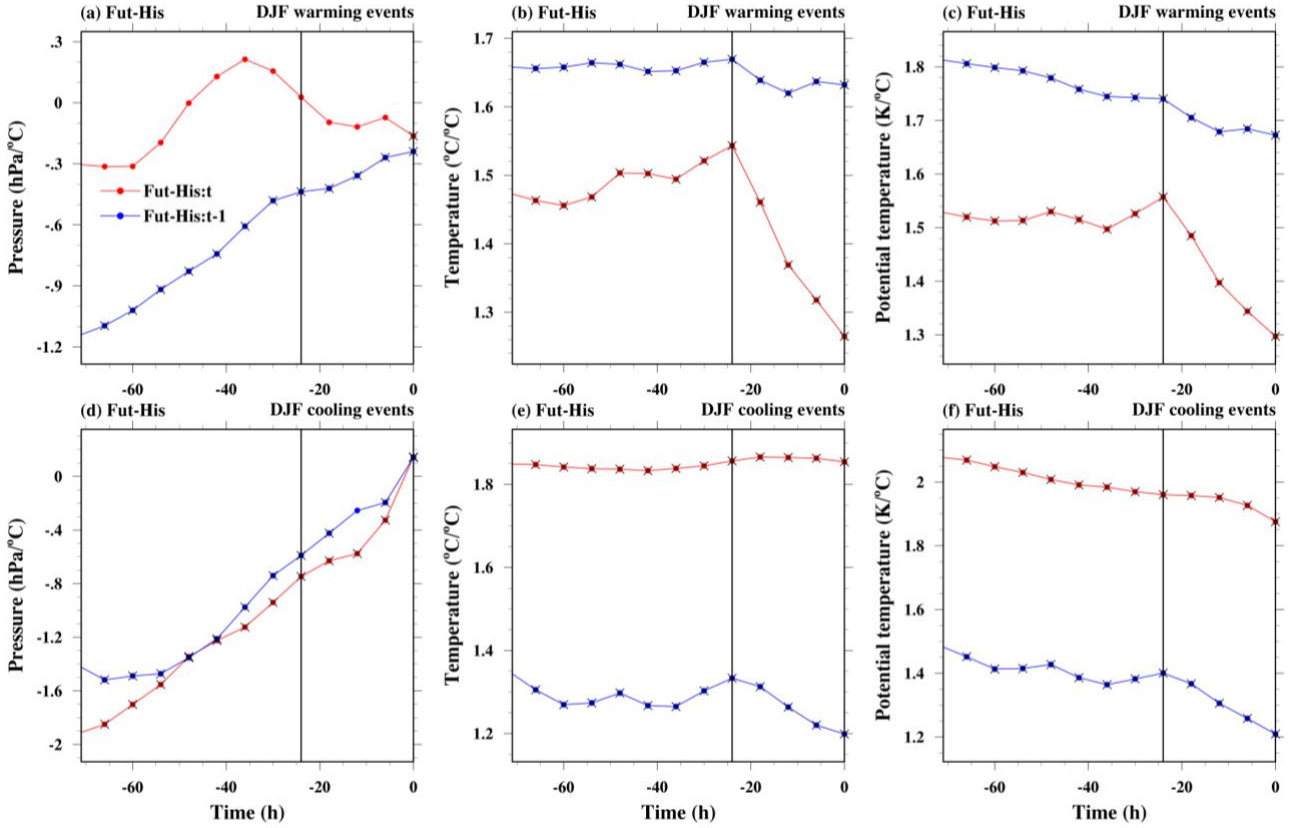


**Figure S6.** The mean Lagrangian evolution of distinct physical parameters: (**a, d**) pressure (hPa), (**b, e**) temperature (°C), and (**c, f**) potential temperature (K) is shown along the air mass trajectories initialised on the previous (*t*–1) and event (*t*) days for projected changes in extremes over North America scaled by annual global surface temperature (°C). Additionally, Bold circles with crosses mark show time steps where the projected changes are statistically significant at the 95 % confidence level based on a t–test.

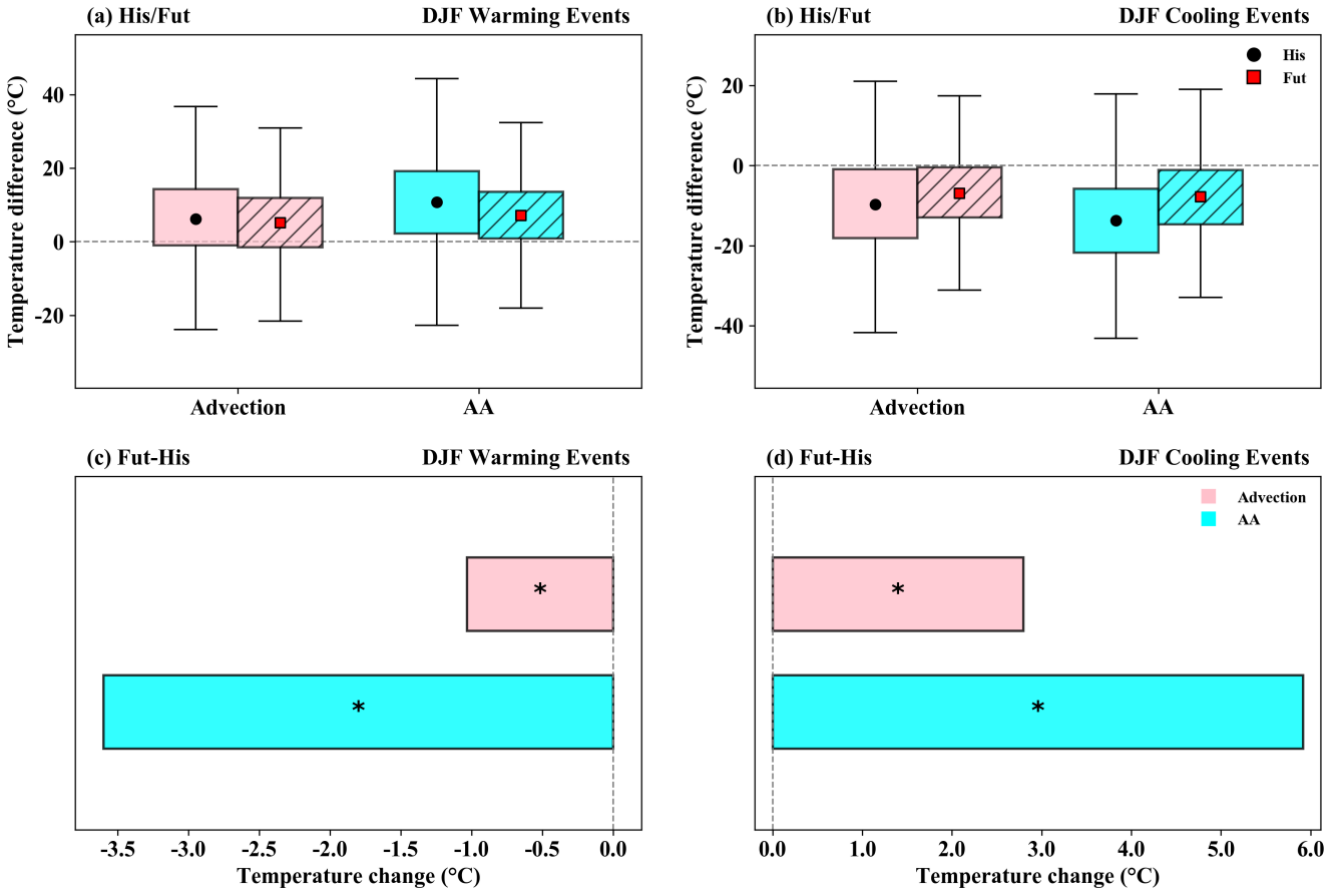


**Figure S7. (a, b)** Box plots comparing the contribution of advection and the estimated effect of Arctic Amplification (AA) for (**a**) warming events and (**b**) cooling events in North America, on a 3 d–time scale. The box spans the 25th and 75th percentiles of the trajectory data; the black dot/red square inside the box gives the mean of the related quantities in the historical/future climate, and the whiskers indicate 1.5 times the interquartile range in panels (**a**) and (**b**). The effect of AA is estimated by comparing the seasonal–mean projected temperature change at the origin (–72 h) for the event day (*t*) and the previous day (*t*–1) along historical backward trajectories. (**c, d**) Stacked horizontal bars showing the mean change (future minus historical) for advection and AA for (**c**) warming and (**d**) cooling events. The * indicates that the difference is statistically significant at the 95 % confidence level based on a t–test.

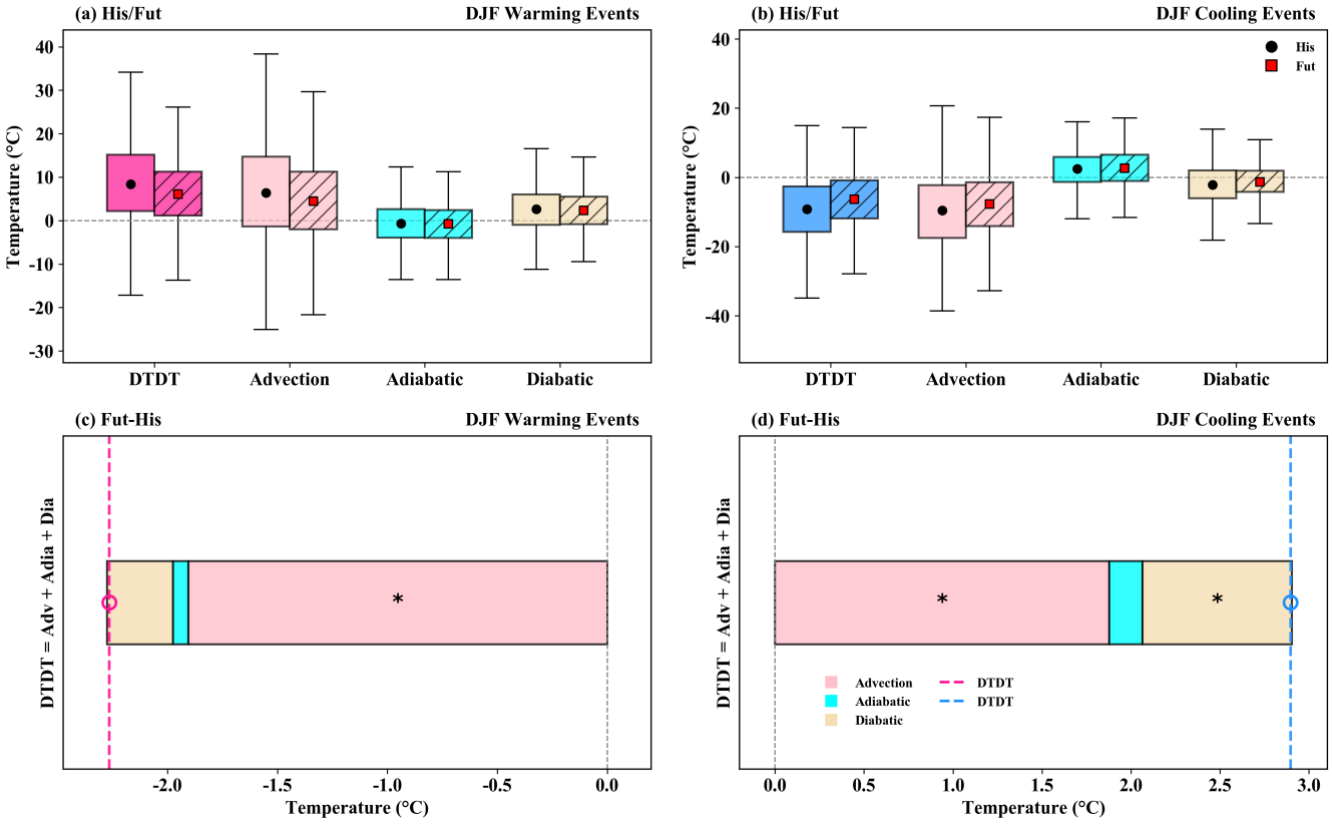


**Figure S8.** The contribution of the different physical processes (advection, adiabatic and diabatic temperature change) over Northern Asia (70°N, 90°E), during December–February (DJF) to the genesis of DTDT (**a, c**) warming and (**b, d**) cooling events during historical/future climate (**a–b**, box plots) and projected change (**c–d**, stacked plots) according to Eq. (2), which refers to a 3 d–time scale. The box spans the 25th and 75th percentiles of the trajectory data; the black dot/red square inside the box gives the mean of the related quantities in the historical/future climate, and the whiskers indicate 1.5 times the interquartile range in panels (**a**) and (**b**). The dotted lines in the stacked plots in panels (**c**) and (**d**) show the mean future change for DTDT warming and cooling events, respectively, and coloured bars indicate the contributions of the individual processes. Circle and * symbols mark future change distributions for which the ensemble means differences exceed the 95% confidence threshold based on a t–test.

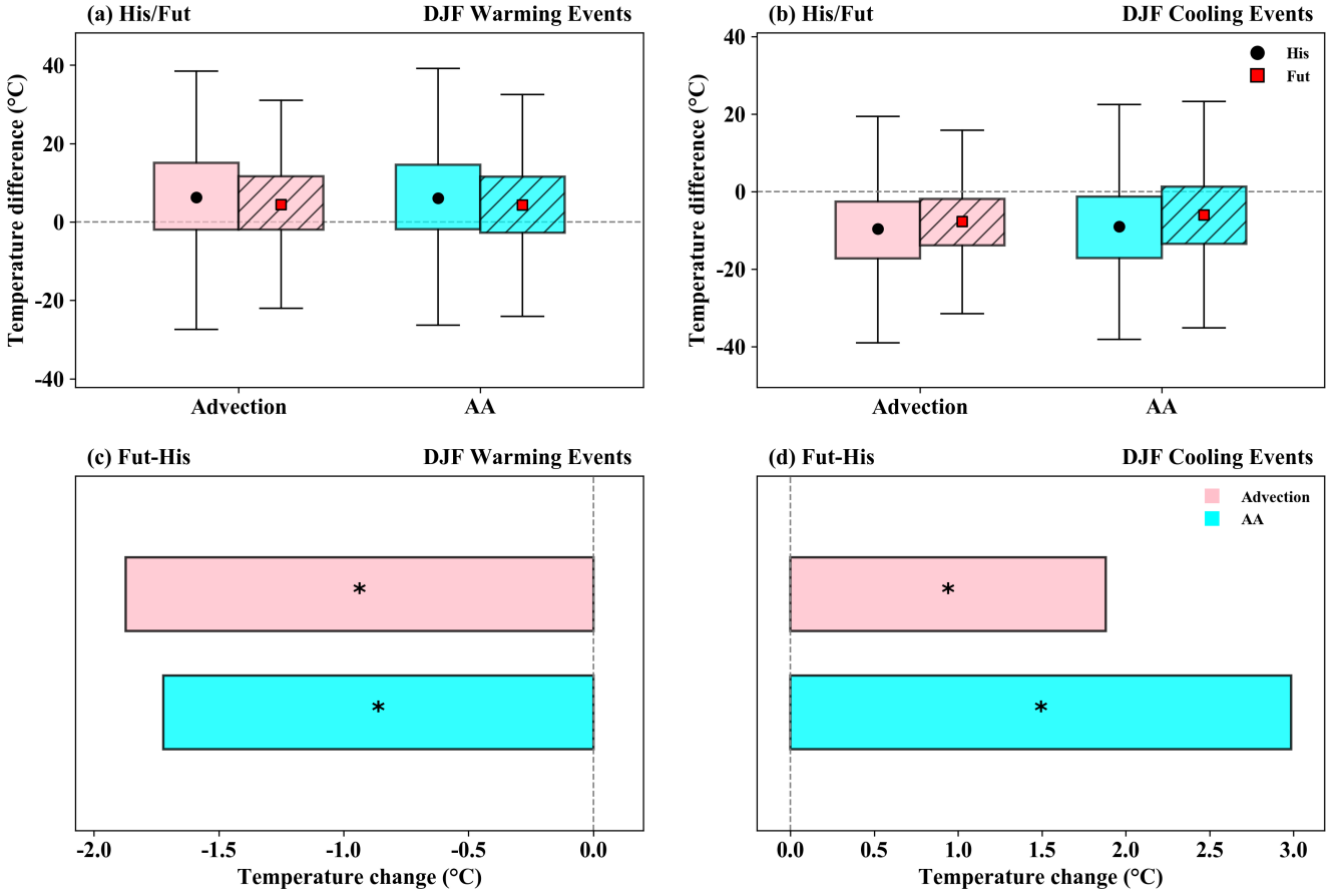


**Figure S9.** (**a, b**) Box plots comparing the contribution of advection and the estimated effect of Arctic Amplification (AA) for (**a**) warming events and (**b**) cooling events in Northern Asia, on a 3 d–time scale. The box spans the 25th and 75th percentiles of the trajectory data; the black dot/red square inside the box gives the mean of the related quantities in the historical/future climate, and the whiskers indicate 1.5 times the interquartile range in panels (**a**) and (**b**). The effect of AA is estimated by comparing the seasonal–mean projected temperature change at the origin (–72 h) for the event day (*t*) and the previous day (*t*–1) along historical backward trajectories. (**c, d**) Stacked horizontal bars showing the mean change (future minus historical) for advection and AA for (**c**) warming and (**d**) cooling events. The * indicates that the difference is statistically significant at the 95 % confidence level based on a t–test.

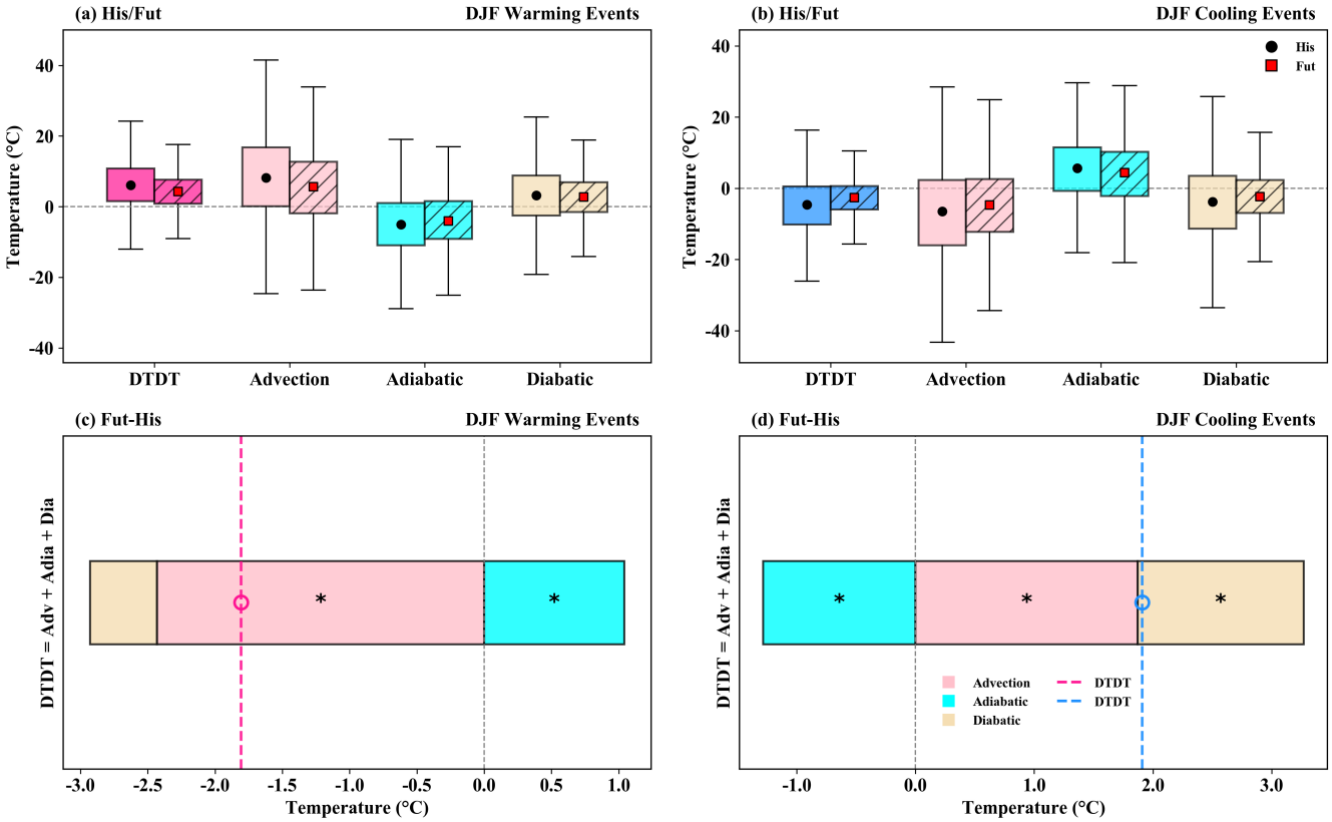


**Figure S10.** The contribution of the different physical processes (advection, adiabatic and diabatic temperature change) over Northern Europe (60°N, 10°E) during December–February (DJF) to the genesis of DTDT (**a, c**) warming and (**b, d**) cooling events during historical/future climate (**a–b**, box plots) and projected change (**c–d**, stacked plots) according to Eq. (2), which refers to a 3 d–time scale. The box spans the 25th and 75th percentiles of the trajectory data; the black dot/red square inside the box gives the mean of the related quantities in the historical/future climate, and the whiskers indicate 1.5 times the interquartile range in panels (**a**) and (**b**). The dotted lines in the stacked plots in panels (**c**) and (**d**) show the mean future change for DTDT warming and cooling events, respectively, and coloured bars indicate the contributions of the individual processes. Circle and * symbols mark future change distributions for which the ensemble means differences exceed the 95% confidence threshold based on a t–test.

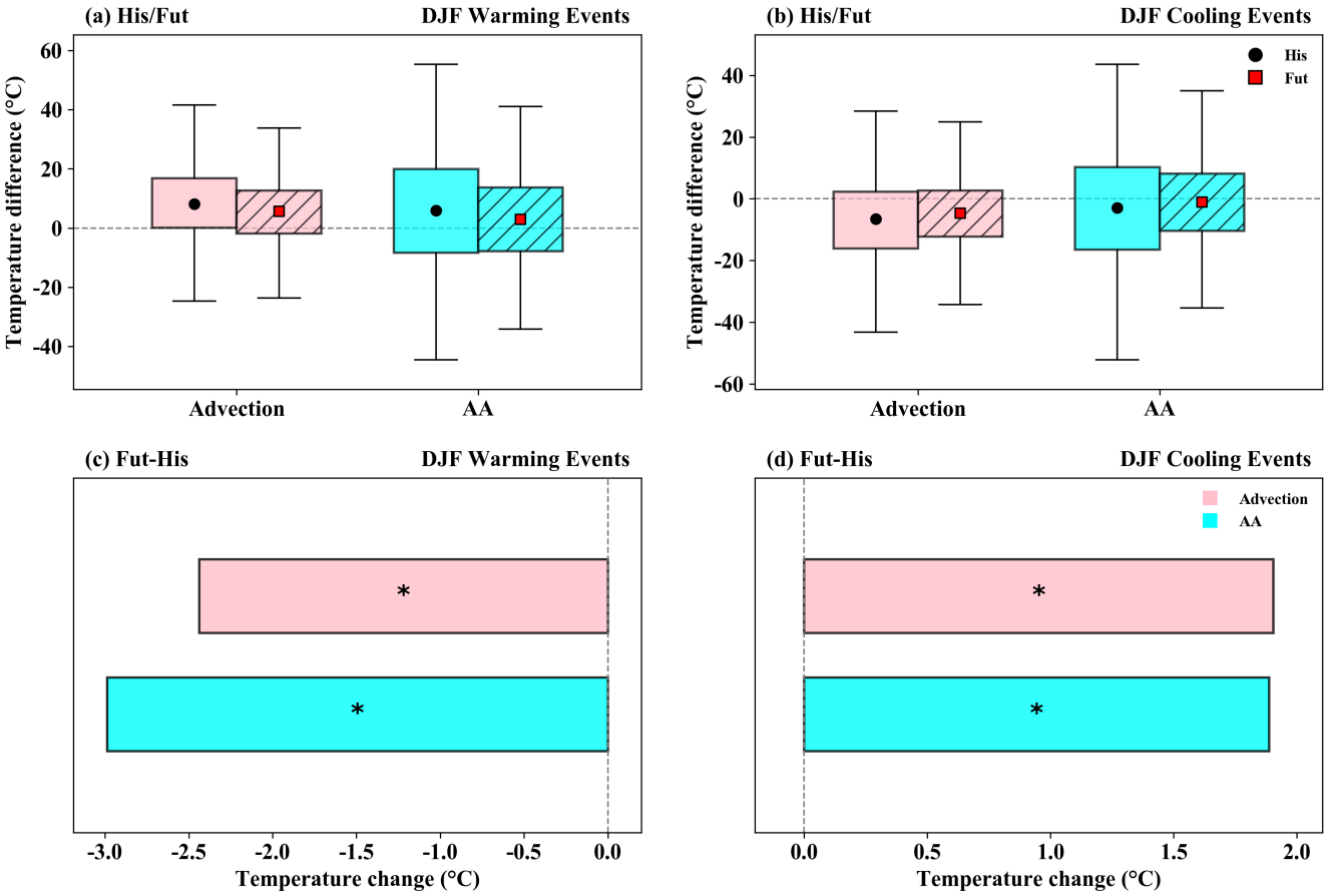


**Figure S11.** (**a, b**) Box plots comparing the contribution of advection and the estimated effect of Arctic Amplification (AA) for (**a**) warming events and (**b**) cooling events in Northern Europe, on a 3 d–time scale. The box spans the 25th and 75th percentiles of the trajectory data; the black dot/red square inside the box gives the mean of the related quantities in the historical/future climate, and the whiskers indicate 1.5 times the interquartile range in panels (**a**) and (**b**). The effect of AA is estimated by comparing the seasonal–mean projected temperature change at the origin (–72 h) for the event day (*t*) and the previous day (*t*–1) along historical backward trajectories. (**c, d**) Stacked horizontal bars showing the mean change (future minus historical) for advection and AA for (**c**) warming and (**d**) cooling events. The * indicates that the difference is statistically significant at the 95 % confidence level based on a t–test.

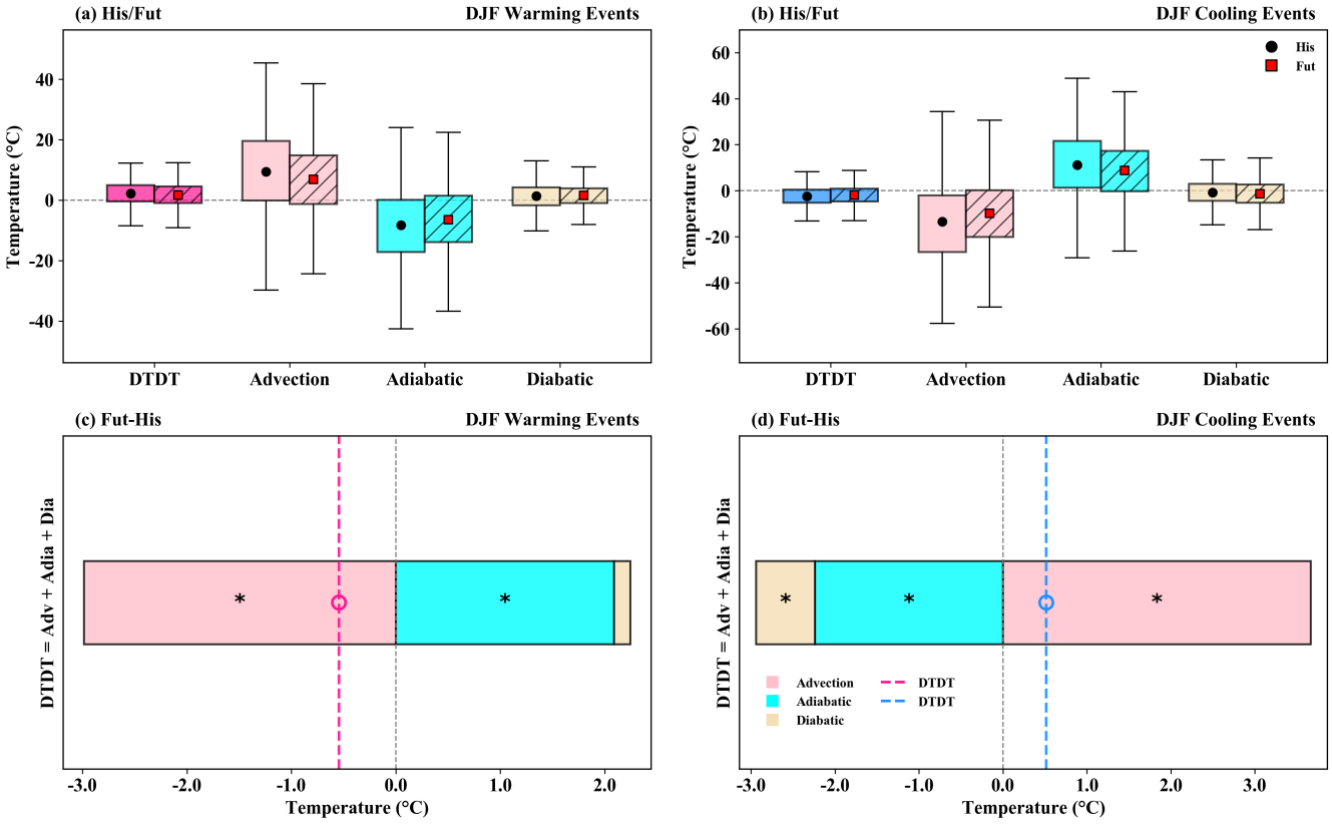


**Figure S12.** The contribution of the different physical processes (advection, adiabatic and diabatic temperature change) over Southern Asia (35°N, 85°E) during December–February (DJF) to the genesis of DTDT (**a, c**) warming and (**b, d**) cooling events during historical/future climate (**a–b**, box plots) and projected change (**c–d**, stacked plots) according to Eq. (2), which refers to a 3 d–time scale. The box spans the 25th and 75th percentiles of the trajectory data; the black dot/red square inside the box gives the mean of the related quantities in the historical/future climate, and the whiskers indicate 1.5 times the interquartile range in panels (**a**) and (**b**). The dotted lines in the stacked plots in panels (**c**) and (**d**) show the mean future change for DTDT warming and cooling events, respectively, and coloured bars indicate the contributions of the individual processes. Circle and * symbols mark future change distributions for which the ensemble means differences exceed the 95% confidence threshold based on a t–test.

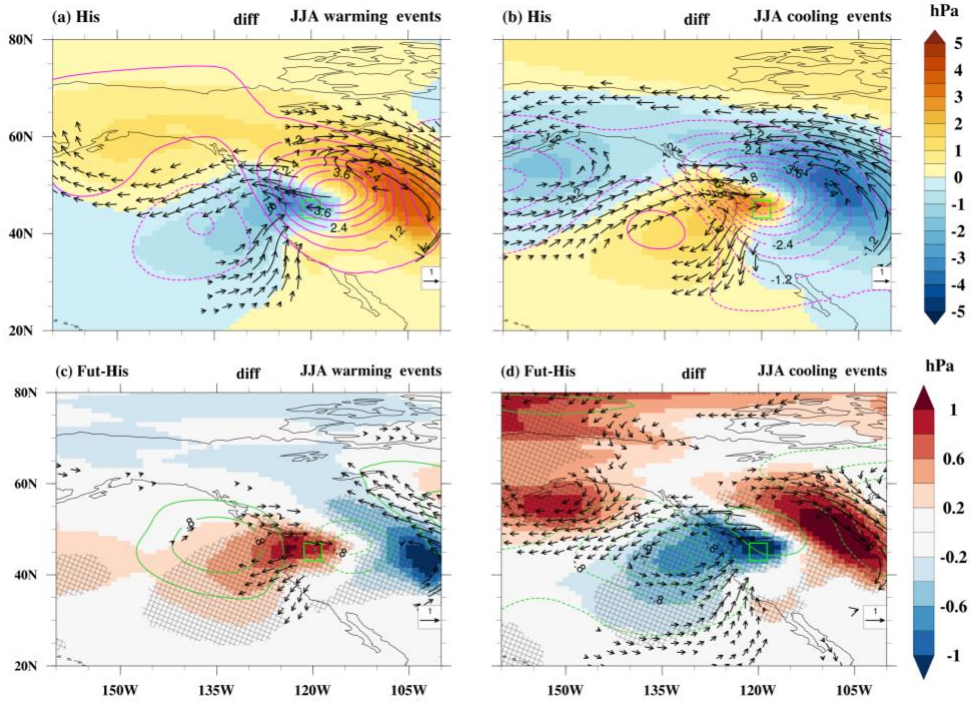


**Figure S13.** Composite difference of absolute sea level pressure (hPa, color shading), wind at 850 hPa (m $s^{-1}$, vectors), and geopotential height 500 hPa (gpm, magenta and darkgreen contours) between the previous day (*t*–1) and event day (*t*) of the warming (**a, c**) and cooling (**b, d**) events during June–August (JJA) in historical climate (His, **a–b**) and projected changes (Fut–His, **c–d**) at a selected grid box in western North America (green box). Note that (in **a–b**) wind vector anomalies ≥0.8 m $s^{-1}$ and (in **c–d**) wind vector anomalies ≥0.2 m $s^{-1}$ are plotted. The bold and dotted contours show increases and decreases of geopotential height, respectively. The hatched area indicates where the ensemble mean of sea level pressure differences (Fut–His) exceeds the 95% confidence threshold based on a t–test.

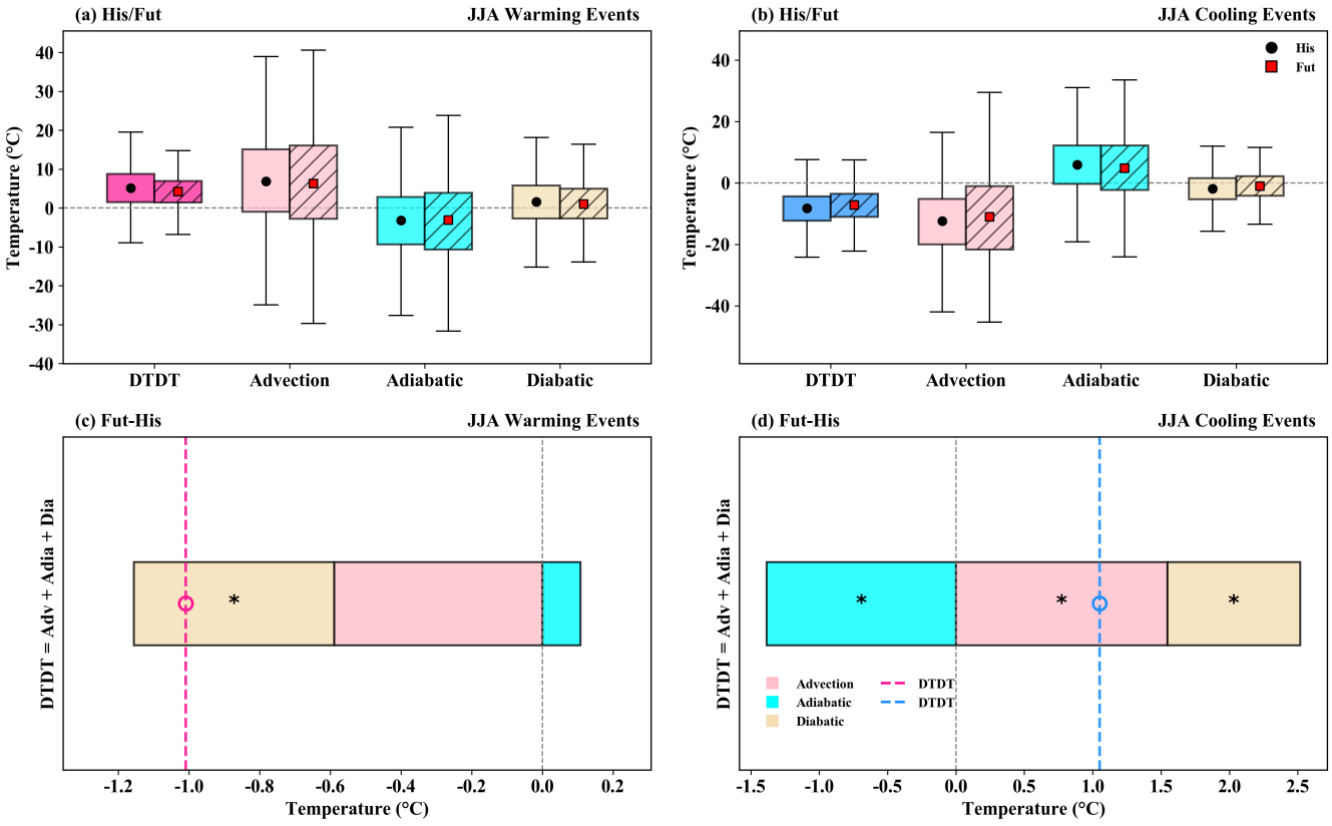


**Figure S14.** The contribution of the different physical processes (advection, adiabatic and diabatic temperature change) over eastern North America (41°N, 76°W) during June–August (JJA) to the genesis of DTDT (**a, c**) warming and (**b, d**) cooling events during historical/future climate (**a–b**, box plots) and projected change (**c–d**, stacked plots) according to Eq. (2), which refers to a 3 d–time scale. The box spans the 25th and 75th percentiles of the trajectory data; the black dot/red square inside the box gives the mean of the related quantities in the historical/future climate, and the whiskers indicate 1.5 times the interquartile range in panels (**a**) and (**b**). The dotted lines in the stacked plots in panels (**c**) and (**d**) show the mean future change for DTDT warming and cooling events, respectively, and coloured bars indicate the contributions of the individual processes. Circle and * symbols mark future change distributions for which the ensemble means differences exceed the 95% confidence threshold based on a t–test.

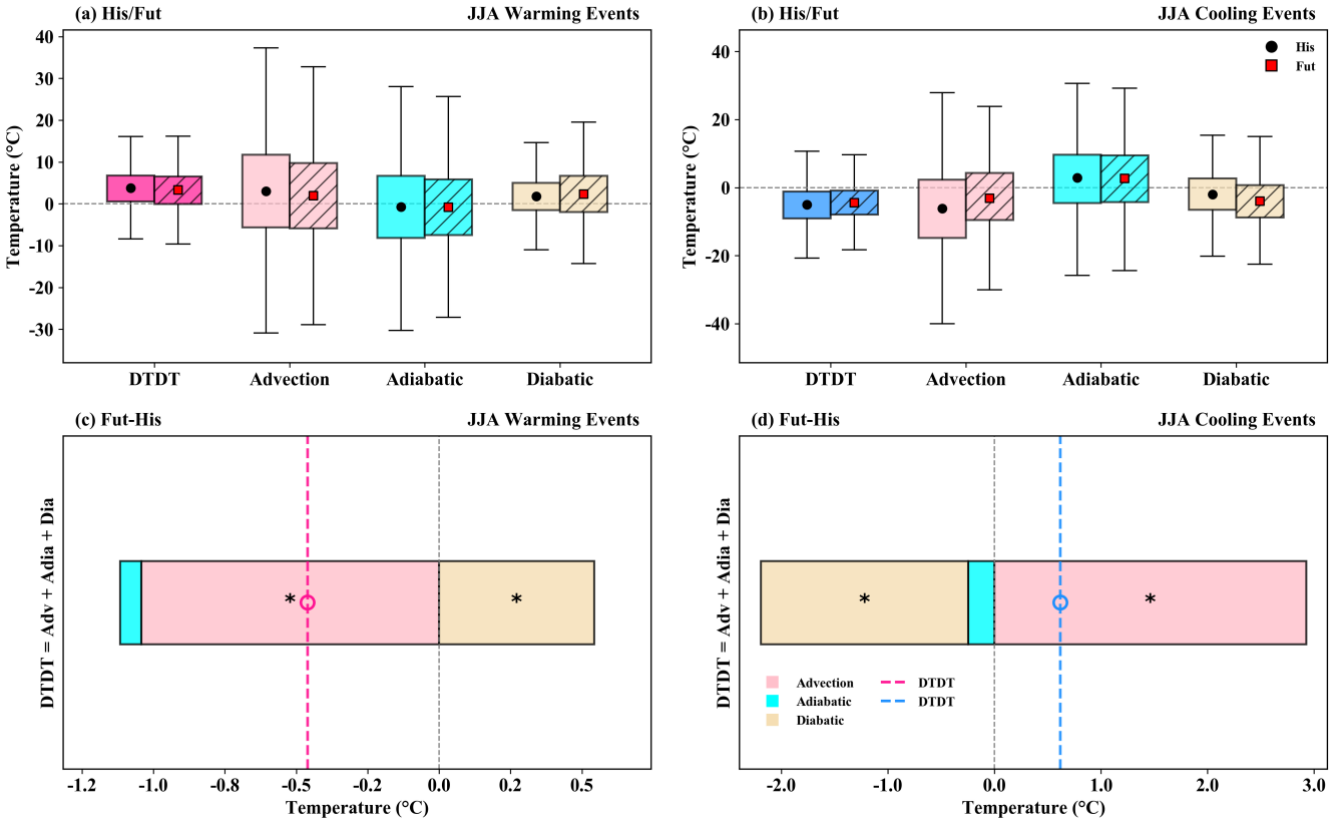


**Figure S15.** The contribution of the different physical processes (advection, adiabatic and diabatic temperature change) over Northeastern Asia (45°N, 50°E) during June–August (JJA) to the genesis of DTDT (**a, c**) warming and (**b, d**) cooling events during historical/future climate (**a–b**, box plots) and projected change (**c–d**, stacked plots) according to Eq. (2), which refers to a 3 d–time scale. The box spans the 25th and 75th percentiles of the trajectory data; the black dot/red square inside the box gives the mean of the related quantities in the historical/future climate, and the whiskers indicate 1.5 times the interquartile range in panels (**a**) and (**b**). The dotted lines in the stacked plots in panels (**c**) and (**d**) show the mean future change for DTDT warming and cooling events, respectively, and coloured bars indicate the contributions of the individual processes. Circle and * symbols mark future change distributions for which the ensemble means differences exceed the 95% confidence threshold based on a t–test.

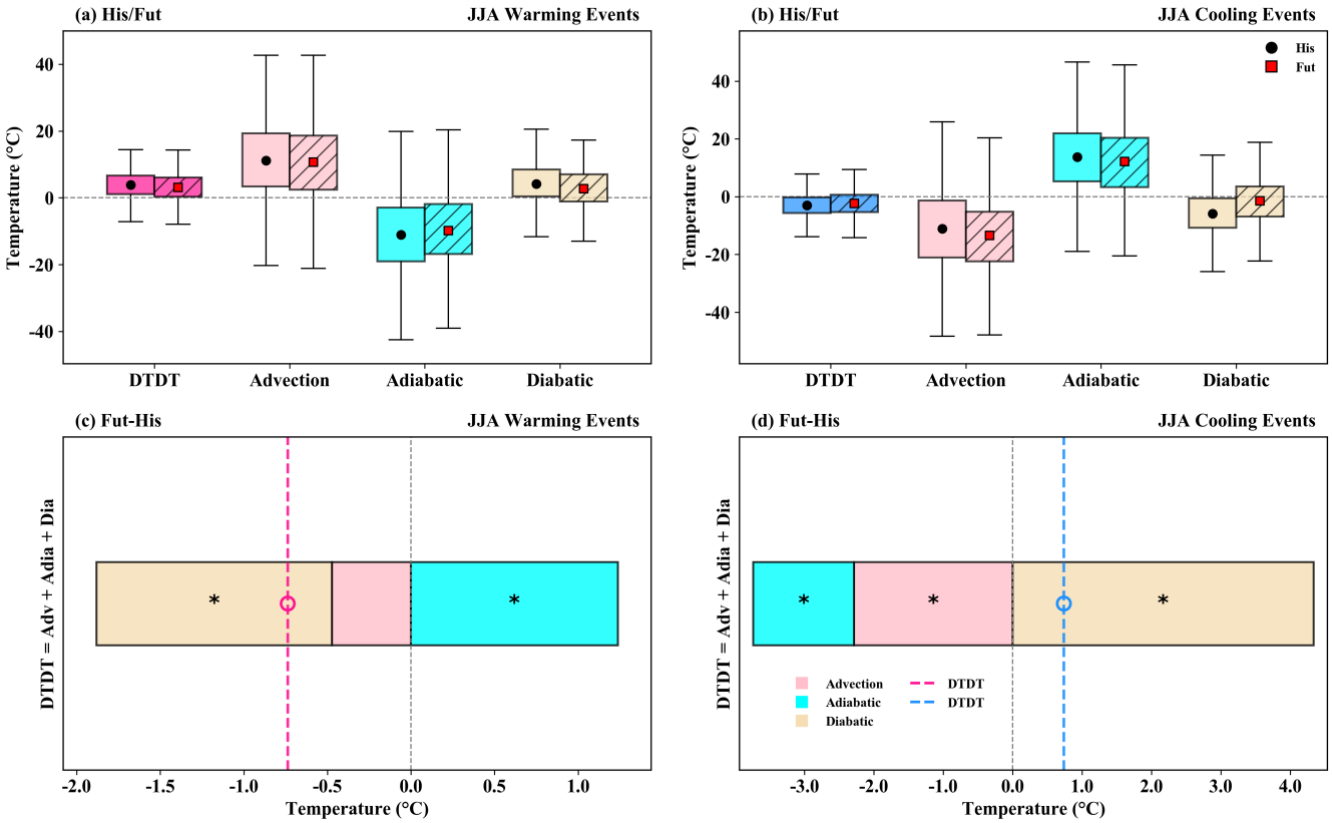


**Figure S16.** The contribution of the different physical processes (advection, adiabatic and diabatic temperature change) over Southern South America (47°S, 70°W) during June–August (JJA) to the genesis of DTDT (**a, c**) warming and (**b, d**) cooling events during historical/future climate (**a–b**, box plots) and projected change (**c–d**, stacked plots) according to Eq. (2), which refers to a 3 d–time scale. The box spans the 25th and 75th percentiles of the trajectory data; the black dot/red square inside the box gives the mean of the related quantities in the historical/future climate, and the whiskers indicate 1.5 times the interquartile range in panels (**a**) and (**b**). The dotted lines in the stacked plots in panels (**c**) and (**d**) show the mean future change for DTDT warming and cooling events, respectively, and coloured bars indicate the contributions of the individual processes. Circle and * symbols mark future change distributions for which the ensemble means differences exceed the 95% confidence threshold based on a t–test.

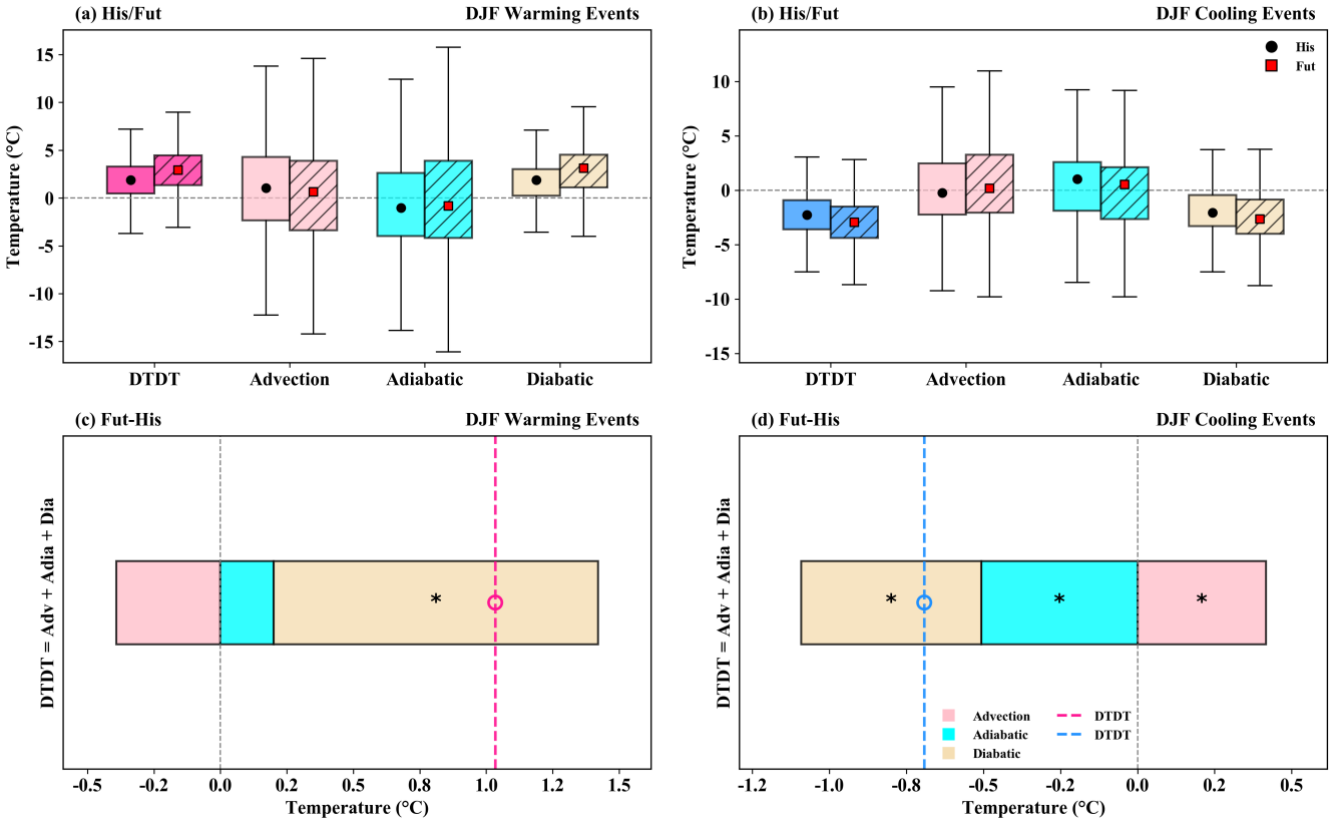


**Figure S17.** The contribution of the different physical processes (advection, adiabatic and diabatic temperature change) over tropical Southern Africa (13°S, 24°E) during December–February (DJF) to the genesis of DTDT (**a, c**) warming and (**b, d**) cooling events during historical/future climate (**a–b**, box plots) and projected change (**c–d**, stacked plots) according to Eq. (2), which refers to a 1 d–time scale. The box spans the 25th and 75th percentiles of the trajectory data; the black dot/red square inside the box gives the mean of the related quantities in the historical/future climate, and the whiskers indicate 1.5 times the interquartile range in panels (**a**) and (**b**). The dotted lines in the stacked plots in panels (**c**) and (**d**) show the mean future change for DTDT warming and cooling events, respectively, and coloured bars indicate the contributions of the individual processes. Circle and * symbols mark future change distributions for which the ensemble means differences exceed the 95% confidence threshold based on a t–test.

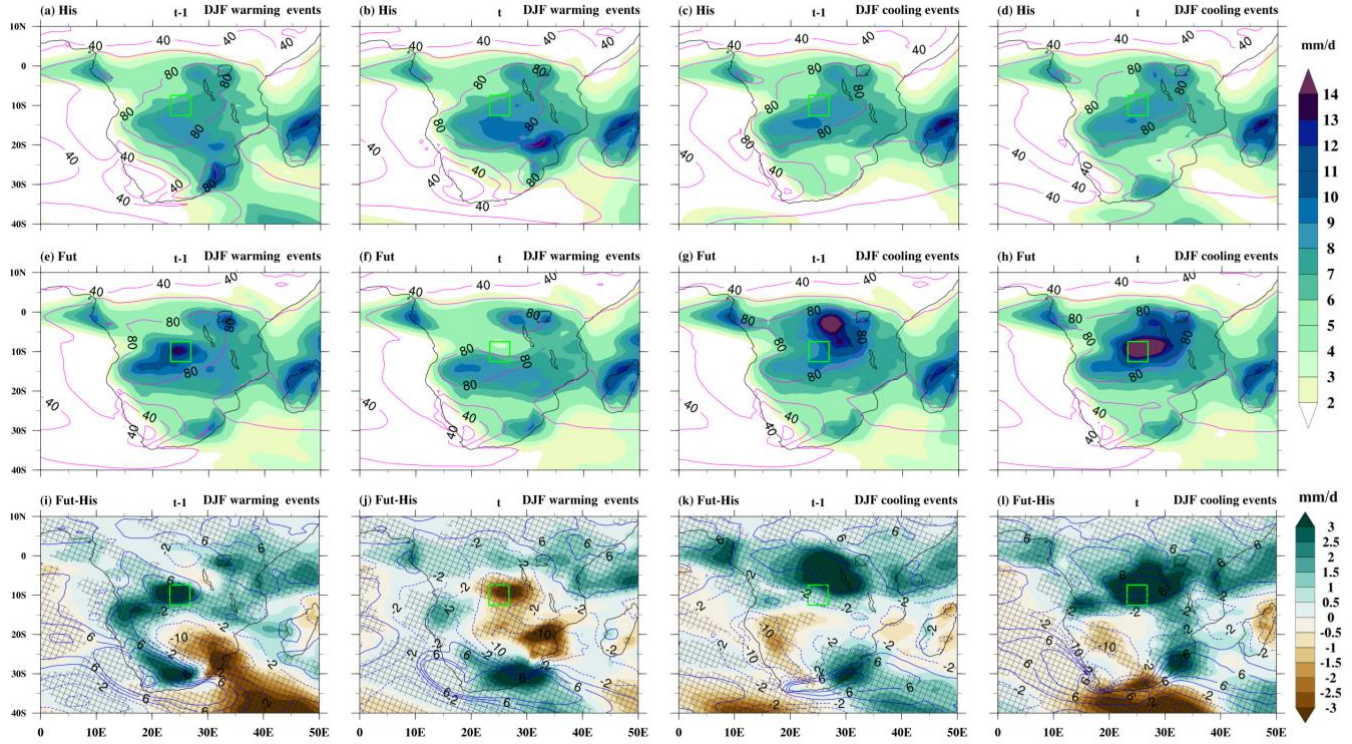


**Figure S18.** Composite of absolute total precipitation (mm $d^{-1}$, colour shading) and total cloud cover (%, magenta and blue contours) on the previous (*t*–1) and event (*t*) days of warming and cooling events during December–February (DJF) over tropical Southern Africa. The top panel displays ensemble means for the (**a–d**) historical climate (His), (**e–h**) future climate (Fut), and (**i–l**) projected change (Fut–His). The green box represents the study grid box, and the crossing–hatching area in (**i–l**) indicates that the ensemble mean of the total precipitation differences exceeds the 95% confidence threshold based on a t–test. The green and brown shading illustrates the increase and decrease in total precipitation, while blue bold and dotted contours represent the increase and decrease in total cloud cover (in Figures **i–l**).

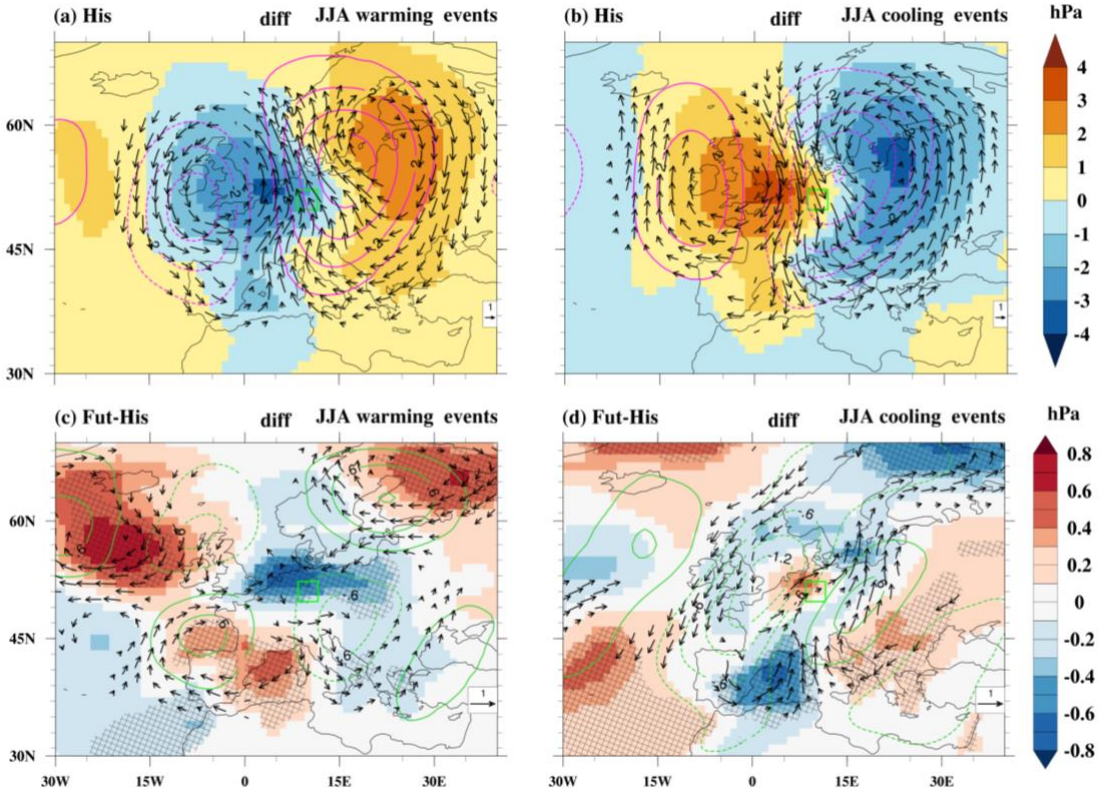


**Figure S19.** Composite difference of absolute sea level pressure (hPa, color shading), wind at 850 hPa (m $s^{-1}$, vectors), and geopotential height 500 hPa (gpm, magenta and darkgreen contours) between the previous day (*t*–1) and event day (*t*) of the warming (**a, c**) and cooling (**b, d**) events during June–August (JJA) in historical climate (His, **a–b**) and projected changes (Fut–His, **c–d**) at a selected grid box in central Europe (green box). Note that (in **a–b**) wind vector anomalies ≥1.2 m $s^{-1}$ and (in **c–d**) wind vector anomalies ≥0.6 m $s^{-1}$ are plotted. The bold and dotted contours show increases and decreases of geopotential height, respectively. The cross–hatching area indicates where the ensemble mean of sea level pressure differences (Fut–His) exceeds the 95% confidence threshold based on a t–test.

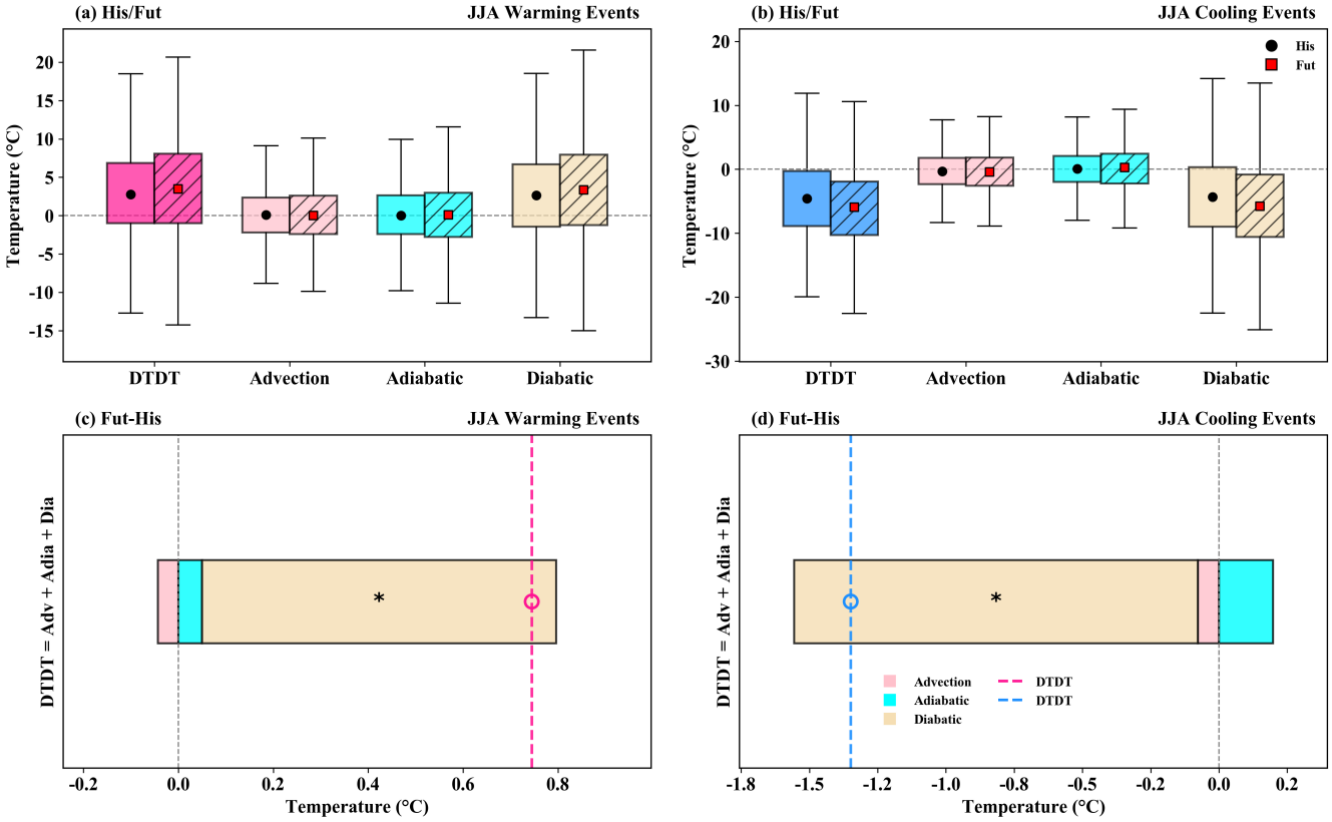


**Figure S20.** The contribution of the different physical processes (advection, adiabatic and diabatic temperature change) over Southern Asia (35°N, 80°E) during June–August (JJA) to the genesis of DTDT (**a, c**) warming and (**b, d**) cooling events during historical/future climate (**a–b**, box plots) and projected change (**c–d**, stacked plots) according to Eq. (2), which refers to a 3 d–time scale. The box spans the 25th and 75th percentiles of the trajectory data; the black dot/red square inside the box gives the mean of the related quantities in the historical/future climate, and the whiskers indicate 1.5 times the interquartile range in panels (**a**) and (**b**). The dotted lines in the stacked plots in panels (**c**) and (**d**) show the mean future change for DTDT warming and cooling events, respectively, and coloured bars indicate the contributions of the individual processes. Circle and * symbols mark future change distributions for which the ensemble means differences exceed the 95% confidence threshold based on a t–test.

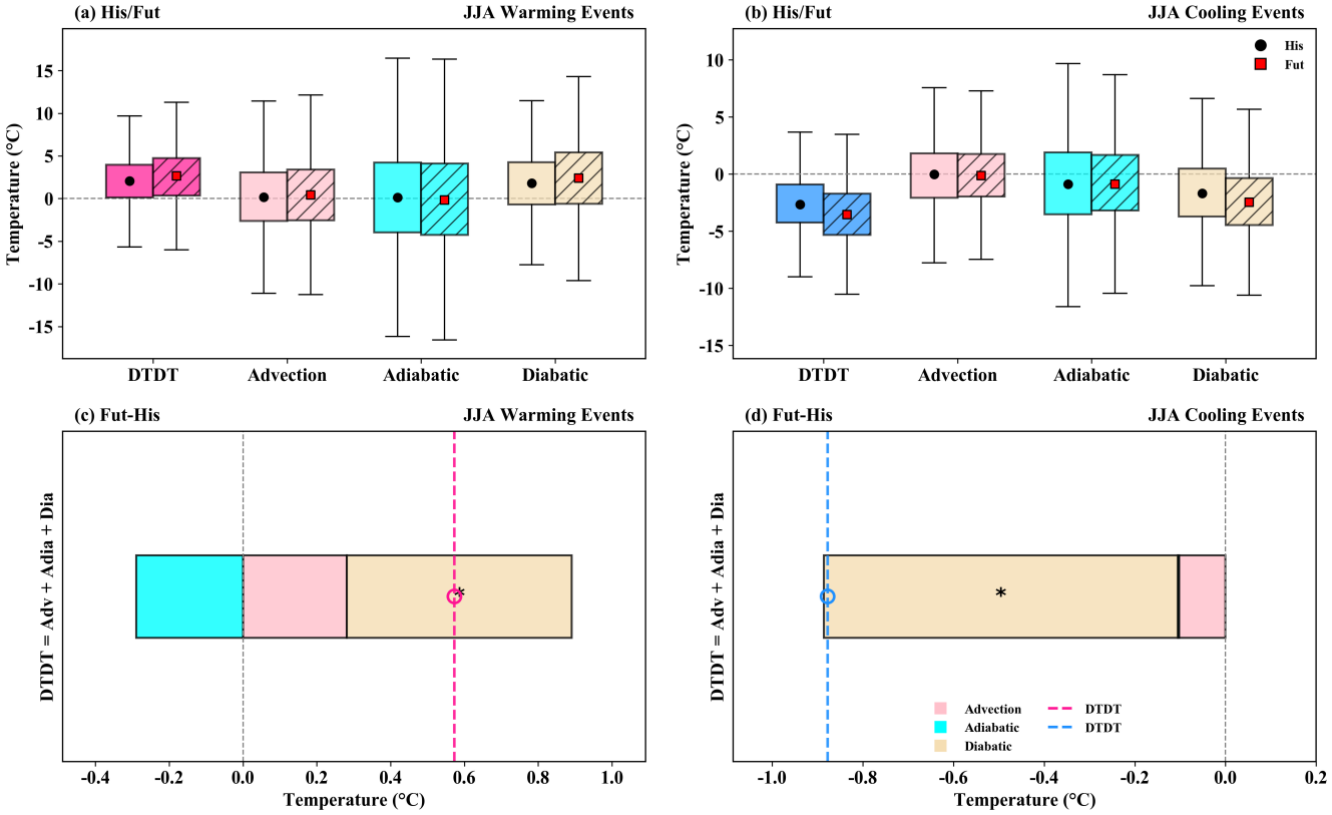


**Figure S21.** The contribution of the different physical processes (advection, adiabatic and diabatic temperature change) over the Sahel region (15°N, 5°E) during June–August (JJA) to the genesis of DTDT (**a, c**) warming and (**b, d**) cooling events during historical/future climate (**a–b**, box plots) and projected change (**c–d**, stacked plots) according to Eq. (2), which refers to a 3 d–time scale. The box spans the 25th and 75th percentiles of the trajectory data; the black dot/red square inside the box gives the mean of the related quantities in the historical/future climate, and the whiskers indicate 1.5 times the interquartile range in panels (**a**) and (**b**). The dotted lines in the stacked plots in panels (**c**) and (**d**) show the mean future change for DTDT warming and cooling events, respectively, and coloured bars indicate the contributions of the individual processes. Circle and * symbols mark future change distributions for which the ensemble means differences exceed the 95% confidence threshold based on a t–test.

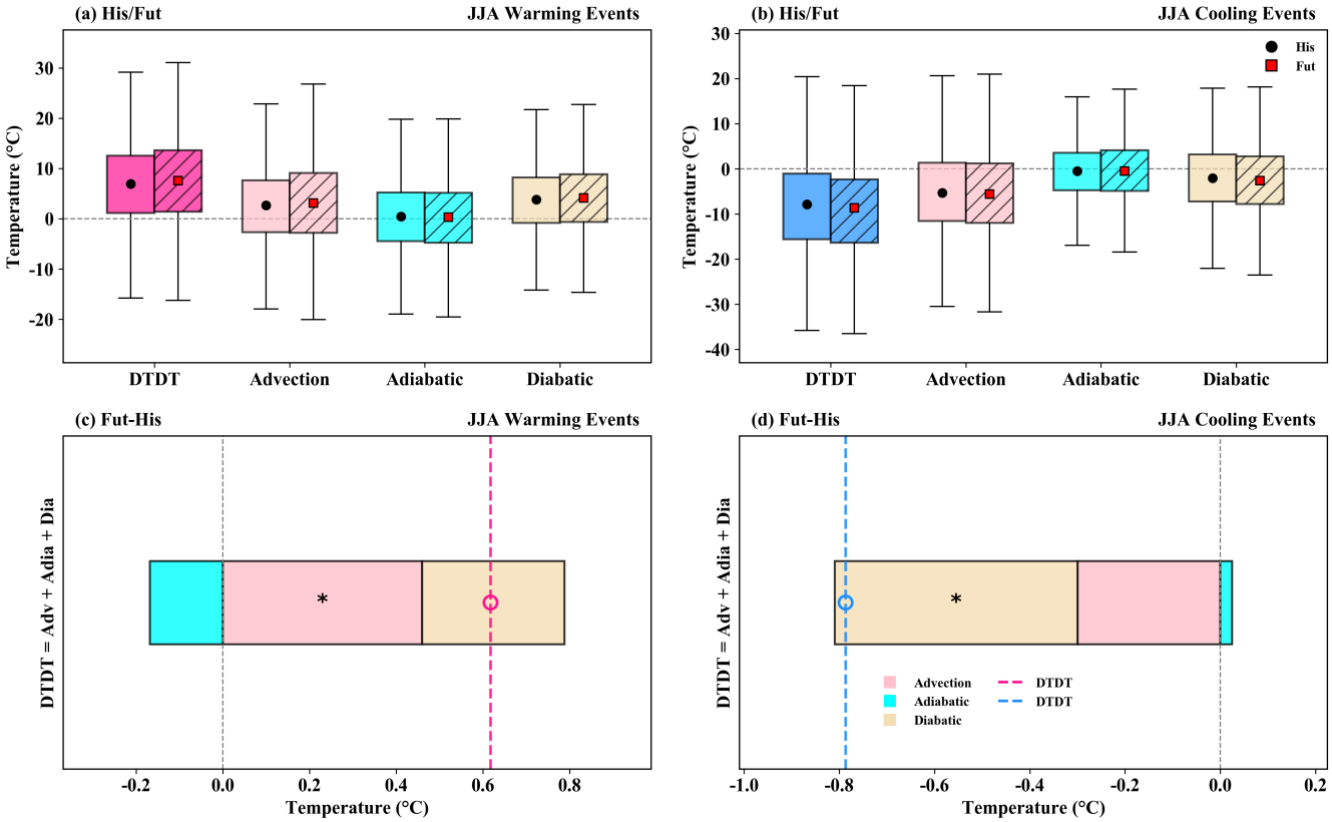


**Figure S22.** The contribution of the different physical processes (advection, adiabatic and diabatic temperature change) over Northern Asia (68°N, 80°E) during June–August (JJA) to the genesis of DTDT (**a, c**) warming and (**b, d**) cooling events during historical/future climate (**a–b**, box plots) and projected change (**c–d**, stacked plots) according to Eq. (2), which refers to a 3 d–time scale. The box spans the 25th and 75th percentiles of the trajectory data; the black dot/red square inside the box gives the mean of the related quantities in the historical/future climate, and the whiskers indicate 1.5 times the interquartile range in panels (**a**) and (**b**). The dotted lines in the stacked plots in panels (**c**) and (**d**) show the mean future change for DTDT warming and cooling events, respectively, and coloured bars indicate the contributions of the individual processes. Circle and * symbols mark future change distributions for which the ensemble means differences exceed the 95% confidence threshold based on a t–test.

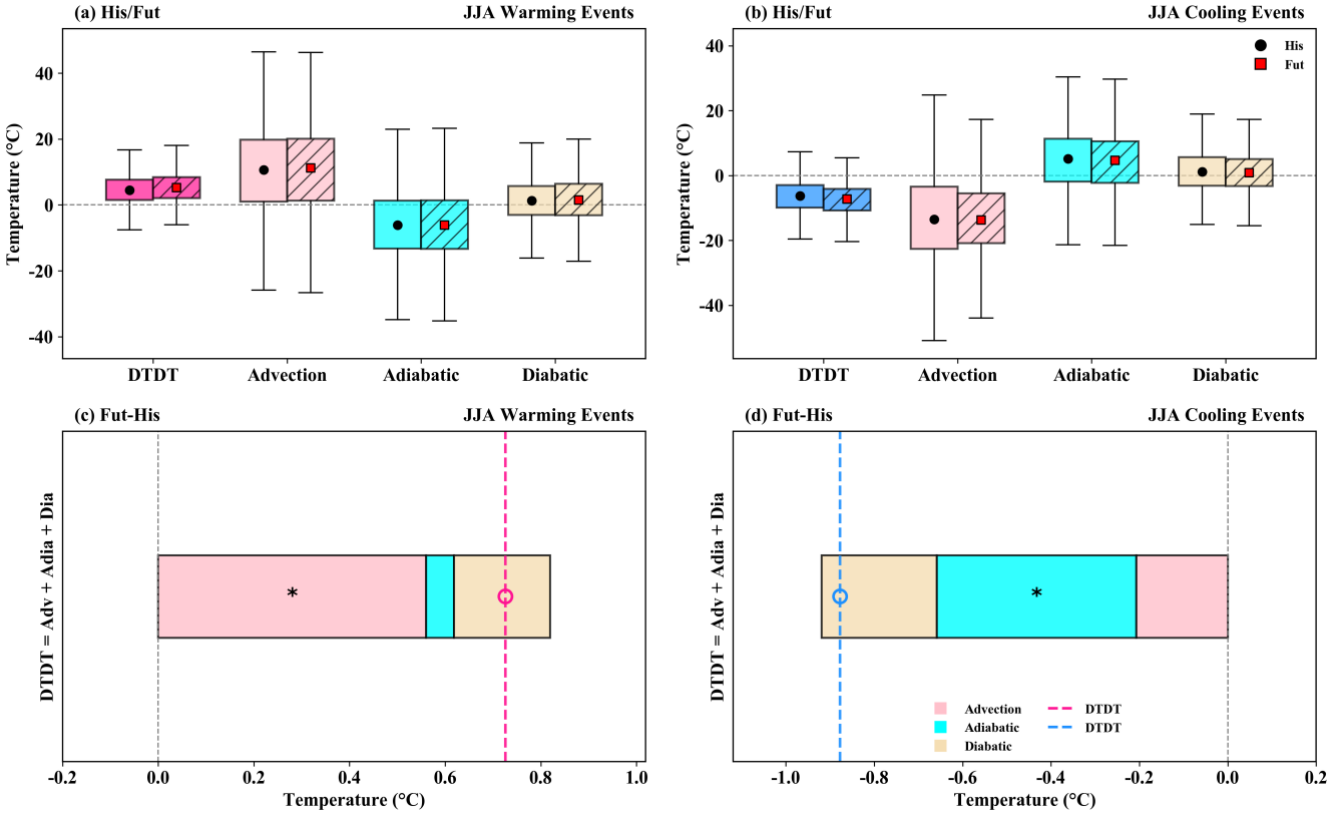


**Figure S23.** The contribution of the different physical processes (advection, adiabatic and diabatic temperature change) over the Southern South Africa (47°S, 70°W) during June–August (JJA) to the genesis of DTDT (**a, c**) warming and (**b, d**) cooling events during historical/future climate (**a–b**, box plots) and projected change (**c–d**, stacked plots) according to Eq. (2), which refers to a 3 d–time scale. The box spans the 25th and 75th percentiles of the trajectory data; the black dot/red square inside the box gives the mean of the related quantities in the historical/future climate, and the whiskers indicate 1.5 times the interquartile range in panels (**a**) and (**b**). The dotted lines in the stacked plots in panels (**c**) and (**d**) show the mean future change for DTDT warming and cooling events, respectively, and coloured bars indicate the contributions of the individual processes. Circle and * symbols mark future change distributions for which the ensemble means differences exceed the 95% confidence threshold based on a t–test.

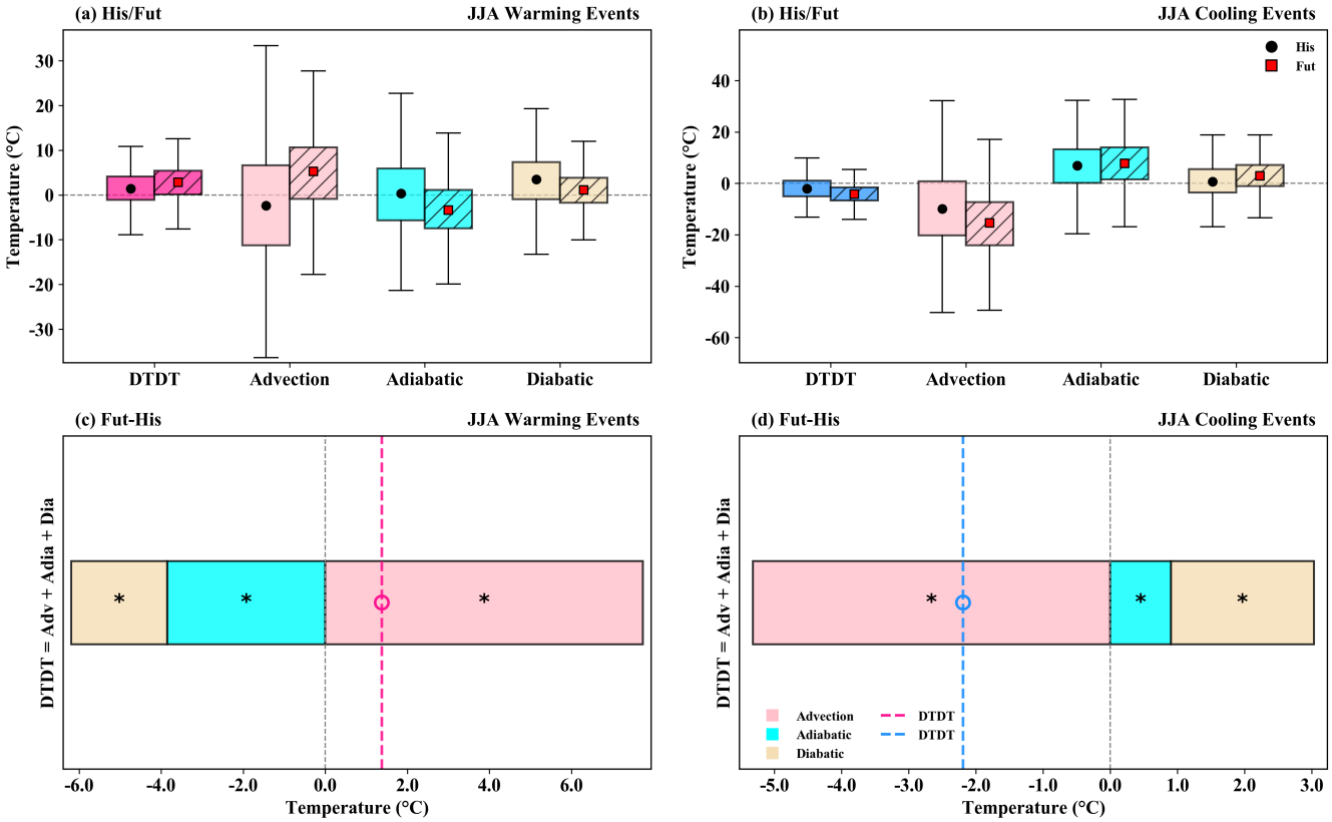


**Figure S24.** The contribution of the different physical processes (advection, adiabatic and diabatic temperature change) over southern Australia (37°S, 140°E) during June–August (JJA) to the genesis of DTDT (**a, c**) warming and (**b, d**) cooling events during historical/future climate (**a–b**, box plots) and projected change (**c–d**, stacked plots) according to Eq. (2), which refers to a 3 d–time scale. The box spans the 25th and 75th percentiles of the trajectory data; the black dot/red square inside the box gives the mean of the related quantities in the historical/future climate, and the whiskers indicate 1.5 times the interquartile range in panels (**a**) and (**b**). The dotted lines in the stacked plots in panels (**c**) and (**d**) show the mean future change for DTDT warming and cooling events, respectively, and coloured bars indicate the contributions of the individual processes. Circle and * symbols mark future change distributions for which the ensemble means differences exceed the 95% confidence threshold based on a t–test.